

# Pareto Actor-Critic for Equilibrium Selection in Multi-Agent Reinforcement Learning

Filippos Christianos\*, Georgios Papoudakis\*, Stefano V. Albrecht

School of Informatics  
The University of Edinburgh  
{f.christianos, g.papoudakis, s.albrecht}@ed.ac.uk

## Abstract

Equilibrium selection in multi-agent games refers to the problem of selecting a Pareto-optimal equilibrium. It has been shown that many state-of-the-art multi-agent reinforcement learning (MARL) algorithms are prone to converging to Pareto-dominated equilibria due to the uncertainty each agent has about the policy of the other agents during training. To address suboptimal equilibrium selection, we propose Pareto-AC (PAC), an actor-critic algorithm that utilises a simple principle of no-conflict games (a superset of cooperative games with identical rewards): each agent can assume the others will choose actions that will lead to a Pareto-optimal equilibrium. We evaluate PAC in a diverse set of multi-agent games and show that it converges to higher episodic returns compared to alternative MARL algorithms, as well as successfully converging to a Pareto-optimal equilibrium in a range of matrix games. Finally, we propose a graph neural network extension which is shown to efficiently scale in games with up to 15 agents.

## 1 Introduction

Multi-agent reinforcement learning (MARL) in *no-conflict games* (a superset of cooperative games, detailed below) aims to jointly train multiple agents to solve a common task in a shared environment. Recent work has focused on reward decomposition (Rashid et al. 2018), communication (Rangwala and Williams 2020), agent modelling (Albrecht and Stone 2018), experience/parameter sharing (Christianos, Schäfer, and Albrecht 2020; Christianos et al. 2021), and more. However, as we will discuss, many of these approaches do not differentiate between multiple Nash equilibria, and are prone to converging to suboptimal equilibria.

Consider the stag hunt game (Table 1), which is an ordinal, no-conflict game with two agents. In an ordinal game, each agent ranks each of the possible outcomes in terms of preference, and in a no-conflict game, all agents have the same set of most-preferred outcomes (Rapoport 1966). Stag hunt is an example of a game with two pure-strategy Nash equilibria,<sup>1</sup> one that is Pareto-optimal and one that is Pareto-dominated (we also refer to it as *risk-averse*) (Harsanyi, Sel-

\*These authors contributed equally.

<sup>1</sup>The stag hunt also has one mixed-strategy Nash equilibrium. However, no-conflict games always have *pure-strategy* Pareto-optimal Nash equilibria. For this reason, in the text, we focus our explanations on pure-strategy equilibria.

		Agent 2	
		A	B
Agent 1	A	(4, 4) <sup>‡</sup>	(0, 3)
	B	(3, 0)	(2, 2) <sup>†</sup>

Table 1: Normal-form of the stag hunt game. The game has two pure Nash equilibria, one that is Pareto-dominated<sup>†</sup> (*risk-averse*) and one that is Pareto-optimal<sup>‡</sup>. In this example, if agent 1 chooses action A, it *risks* receiving zero reward if the other agent chooses B. But, if agent 1 chooses action B it will always receive a reward of at least 2.

ten et al. 1988). While the Pareto-optimal equilibrium yields the highest returns for all agents, the risk-averse equilibrium is typically selected when an agent is uncertain of the action of the other agent. Here, *risk* refers to the prospect of an inadvertent selection of a joint action that is penalised. In the context of MARL, the study of Papoudakis et al. (2021) showed that many recent MARL algorithms are unable to converge to the Pareto-optimal equilibrium in the Penalty and Climbing matrix games (see Section 4.1) used by Claus and Boutilier (1998). We corroborate these findings by showing the tendency of MARL algorithms to converge to a risk-averse equilibrium in stateless matrix games. Furthermore, we show that this behaviour can extend to sequential state-based games if they contain suboptimal equilibria in the form of penalties for failing to coordinate.

The reason MARL algorithms, such as QMIX (Rashid et al. 2018) or IPPO (Schulman et al. 2017), converge to Pareto-dominated equilibria is rooted in the exploration policies used to explore the state-action space (e.g., using  $\epsilon$ -greedy or soft policies). For example, policy gradient algorithms sample actions from the stochastic policy they learn. When the training starts, the stochastic policies are almost uniform, and often dominated by an entropy term used to promote exploration (Mnih et al. 2016). Therefore, during the early stages of training, agents quickly learn that risky actions are penalised, which makes them assign probability mass to less risky actions. However, this further reinforces the risk-averse equilibrium in a feedback loop. We aim to address this issue by modifying the reinforcement learning objective in a way that keeps exploring actions even if they are risky.

We propose an algorithm, called *Pareto Actor-Critic (PAC)*,

which is designed to converge to pure-strategy Pareto-optimal Nash equilibria in no-conflict games. The algorithm makes use of the fact that in no-conflict games, all agents know that the Pareto-optimal equilibrium is also preferred by all the other agents. To do so, the algorithm guides the policy gradient to the Pareto-optimal equilibrium by using a modified advantage estimation that takes into account the assumption that each agent can “trust” the other agents to choose the action that leads to the same equilibrium. PAC is shown to work in environments with high-dimensionality while still adhering to the centralised-training decentralised-execution (CTDE) paradigm. Moreover, to enable scaling to a larger number of agents (up to 15 in our experiments), we show how PAC can use tractable graph-based approximations (Böhmer, Kurin, and Whiteson 2020).

In summary, we contribute a novel deep MARL algorithm which i) successfully converges to Pareto-optimal pure Nash equilibria in all 21 distinct  $2 \times 2$  no-conflict matrix games (Rapoport 1966) and three larger matrix-games (Claus and Boutilier 1998), ii) learns to coordinate in partially observable stochastic games with higher dimensionality and converges to higher overall returns than state-of-the-art MARL algorithms (even learning in environments where other algorithms fail), even when doing so is risky, iii) adheres to the CTDE paradigm that is commonly used in MARL research, and iv) can be scaled to many agents using the proposed PAC-DCG graph-based approach.

## 2 Technical Preliminaries

### 2.1 Partially Observable Stochastic Games

We consider a Partially Observable Stochastic Game (POSG) (Hansen, Bernstein, and Zilberstein 2004) which is defined by  $(\mathcal{I}, \mathcal{S}, \mathcal{O}, \mathcal{A}, \Omega, \mathcal{P}, \mathcal{R})$ , where  $\mathcal{I}$  is the set of  $N$  agents  $i \in \mathcal{I} = \{1, \dots, N\}$ ,  $\mathcal{S}$  is the set of states of the game,  $\mathcal{A} = A^1 \times \dots \times A^N$  is the set of joint actions, where  $A^i$  is the action set of agent  $i$ , and  $\mathcal{O} = O^1 \times \dots \times O^N$  is the joint observation set.  $\Omega : \mathcal{S} \times \mathcal{A} \times \mathcal{O} \rightarrow [0, 1]$  and  $\mathcal{P} : \mathcal{S} \times \mathcal{A} \times \mathcal{S} \rightarrow [0, 1]$  are probability distributions over the joint next observation and next state, respectively, given the current state and joint action. Finally,  $\mathcal{R} : \mathcal{S} \times \mathcal{A} \times \mathcal{S} \rightarrow \mathbb{R}^N$  is the reward function that returns a reward  $r^i$  for each agent  $i$ . The objective of each agent  $i$  is to find a policy  $\pi^i$  that maximises its expected sum of discounted rewards given the policy of all other agents  $\pi^{-i}$ :

$$\pi^i \in \arg \max_{\pi^i} \mathbb{E} \left[ \sum_{t=0}^{H-1} \gamma^t r_t^i | \pi^i, \pi^{-i} \right]$$

where  $\gamma \in [0, 1]$  is the discount factor, and  $H$  is the horizon of the episode.

### 2.2 Policy Gradient and Actor-Critic

Policy gradient methods aim to find the parameters  $\phi$  of the parameterised policy  $\pi_\phi$  that maximise the expectation, under the parameterised policy, of the discounted sum of rewards for the duration of episode. The simplest policy gradient method is REINFORCE (Williams 1992), which, in single-agent RL, estimates the gradient of the objective

$J(\phi) = \mathbb{E}_\pi [G_t \nabla_\phi \log \pi_\phi(a_t | s_t)]$ , where  $G_t$  is the Monte-Carlo return estimation. To minimise the variance of the gradient estimation in REINFORCE, we (i) subtract the state value from the returns, and (ii) approximate the returns using the state value function. Therefore, we also need to learn a function that approximates the state value function  $V_\theta$  with parameters  $\theta$ . The class of algorithms that learn both a policy and a value function is called actor-critic. The most commonly used actor-critic algorithm is advantage actor-critic (A2C) (Mnih et al. 2016). An application of A2C in MARL is the Independent A2C (IA2C) algorithm, where each agent is trained by ignoring the presence of the other agents in the environment, with the actor of agent  $i$  minimising:

$$\mathcal{L}(\phi_i) = -\log \pi(a_t^i | o_t^i; \phi_i) (r_t^i + \gamma V(o_{t+1}^i; \theta_i) - V(o_t^i; \theta_i)) \quad (1)$$

and the critic of agent  $i$  minimising:

$$\mathcal{L}(\theta_i) = (r_t^i + \gamma V(o_{t+1}^i; \theta_i) - V(o_t^i; \theta_i))^2 \quad (2)$$

Extensions of independent actor-critic methods have been proposed by Lowe et al. (2017); Foerster et al. (2018), where the critic is conditioned on the joint trajectory of all agents to better approximate the expected return of each agent. The centralised training version of IA2C, which is often called MAA2C or Central-V, is trained to minimise the following loss for the actor:

$$\mathcal{L}(\phi_i) = -\log \pi(a_t^i | o_t^i; \phi_i) (r_t^i + \gamma V(\mathbf{o}_{t+1}; \theta_i) - V(\mathbf{o}_t; \theta_i)) \quad (3)$$

and for the critic minimising:

$$\mathcal{L}(\theta_i) = (r_t^i + \gamma V(\mathbf{o}_{t+1}; \theta_i) - V(\mathbf{o}_t; \theta_i))^2 \quad (4)$$

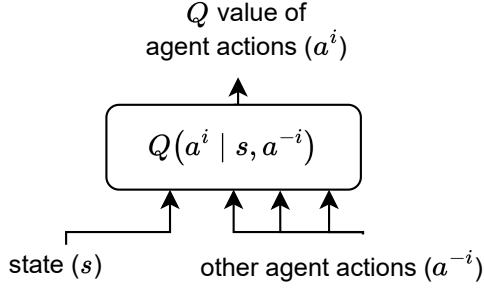
for each agent  $i$ , where  $\mathbf{o}$  is the joint observation of all agents.

## 3 Pareto Actor-Critic Algorithm

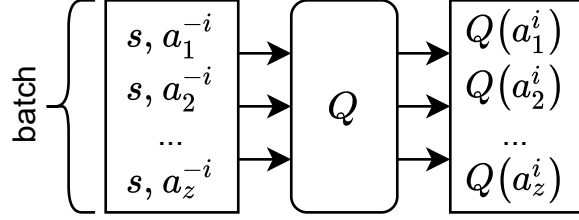
Revisiting the stag hunt of Table 1, we observe that agents can reach the desired Pareto-optimal equilibrium if they both coordinate. There is no incentive for any of the agents to deviate from that equilibrium, and if we assume that this is known by both, the agents can select action  $A$ . We make use of this property while preserving the decentralised interaction of each agent with the environment. To do so, we use an actor-critic architecture in which the critic requires centralised training while the actor selects actions in a decentralised fashion.

### 3.1 Methodology

To allow agents to explore and converge to a Pareto-optimal equilibrium, we use a critic that estimates the maximum Q-value over the joint actions of all the other agents  $-i$  from the perspective of agent  $i$ , i.e.  $\max_{a_{-i}} Q(\mathbf{o}_t, a_t^i, a_{-i}^{-i})$ . The max-operator is the core of our approach. Calculating the maximum Q-value over the possible actions of the other agents translates to *assuming* that the other agents will execute that action. Therefore, from the point of view of each agent, the other agents will execute the action that will lead to the Pareto-optimal equilibrium. This is true, because from the definition of no-conflict games, all agents have the same preferred joint action.



(a) The  $Q$  network receives as inputs the state and the actions of the other agents (concatenated together) and outputs a  $Q$  value for each of the discrete actions of agent  $i$ .



(b) The  $Q$  network architecture allows us to compute all the combinations of other agent actions *in parallel*, in a single forward operation.  $z$  is the number of joint actions  $a^{-i}$  for other agents.

Figure 1: PAC  $Q$  network architecture and parallel computation.

The number of joint actions scales exponentially in the number of agents in the environment, rendering the computation of the  $Q$ -values of all joint actions computationally expensive. To address this issue, our algorithm includes two distinct design choices (also seen in Figures 1a and 1b).

First, we circumvent a growing critic-network architecture by moving the other agent actions to the input of the network (see Fig. 1a); scaling the network size linearly to the number of agents. Second, we parallelise the computation of  $Q(\mathbf{o}_t, \cdot, a_t^{-i})$  since it scales exponentially with respect to the number of agents. We do so with a critic that receives a batched input that contains the observation concatenated with all the possible  $a^{-i}$ . The combinations of the actions  $a^{-i}$  is the Cartesian product of the action spaces  $A^{-i} = \times_{j \neq i} A^j$  which can then be concatenated with the joint observation of all agents. Using this as the input to the critic-network, all the possible  $Q$  values can be generated in a single forward pass (see Fig. 1b).

By using the above methodology, we can train the critic network. Note that in contrast to common on-policy actor-critic architectures (e.g., A2C and PPO), PAC’s critic approximates the  $Q$ -values instead of the state values. Training the  $Q$ -function can simply be done by minimising the TD-error between the selected actions and the target, which includes the described max-operator:

$$\mathcal{L}(\theta_i) = (r_t^i + \gamma \max_{a^i, a^{-i}} \hat{Q}(\mathbf{o}_{t+1}, a_t^i, a_t^{-i}) - Q(\mathbf{o}_t, a_t^i, a_t^{-i}))^2 \quad (5)$$

with  $\hat{Q}$  being the target network (updated either with hard or soft updates).

We train the critic in a centralised fashion, but still require a way to train a decentralised actor, that converges to the desired equilibria. We modify the policy gradient loss to replace the approximation of returns  $r_t^i + \gamma V(\mathbf{o}_{t+1}^i; \theta_i)$  with the equivalent  $\max_{a^{-i}} Q(\mathbf{o}_t^i, a_t^i, a_t^{-i})$ . Also, actor-critic algorithms typically subtract a baseline from the returns (e.g.  $V(\mathbf{o}_t^i; \theta_i)$ ). Given that we do not train a separate value network, we can simply replace this with the equivalent:

$$V(\mathbf{o}_t; \theta_i) = \sum_{a^i} \pi(a_t^i | \mathbf{o}_t^i; \phi_i) Q(\mathbf{o}_t, a_t^i, a_t^{-i}) \quad (6)$$

Our final policy gradient loss for PAC becomes:

$$\mathcal{L}(\phi_i) = -\log \pi(a_t^i | \mathbf{o}_t^i; \phi_i) (\max_{a^{-i}} Q(\mathbf{o}_t, a_t^i, a_t^{-i}) - \sum_{a^i} \pi(a_t^i | \mathbf{o}_t^i; \phi_i) Q(\mathbf{o}_t, a_t^i, a_t^{-i})) \quad (7)$$

The loss, described in Eq. (7) above, maximises the  $Q$ -values but *ignores* any miscoordination with the rest of the agents. While this loss still requires centralised training, the actor can be used independently since it is only conditioned on the local observation of each agent.

### 3.2 Approximations for Scaling to Many Agents

The architecture proposed allows for efficient computation of  $Q$ -values up to a small number of agents (e.g. up to five). However, the computation becomes prohibitively expensive with a larger number of agents, requiring a batch size that scales exponentially with the number of agents. To enable efficient scaling to more agents, we approximate the max  $Q$ -values via a graph-based representation, specifically Deep Coordination Graphs (DCG) (Böhmer, Kurin, and Whiteson 2020).

Equations (5) and (7) only require the maximum  $Q$ -value of the joint actions, as well as the  $Q$ -values of the specific joint action that is executed at each time step and not the  $Q$ -values of all joint actions. DCG assumes that the  $Q$ -value of a joint action can be factorised using a fully-connected undirected graph, where each node represents an agent that has its own utility function. Each edge between two nodes represents the pairwise payoff function between the two agents. Both the utility functions as well as the payoff functions are approximated using neural networks. The maximum  $Q$ -value of the joint actions can be computed using a message-passing algorithm. Using DCG as critic we can compute the maximum  $Q$ -value with complexity  $\mathcal{O}(k|A|(|A| + N)\mathcal{E})$  (Böhmer, Kurin, and Whiteson 2020), where  $k$  is the number of message passing iterations,  $|A|$  the size of the largest single-agent action space, and  $\mathcal{E}$  the number of edges, in contrast to computing the  $Q$ -values of all joint actions with complexity  $\mathcal{O}(|A|^{N-1})$ . Since we do not have access to the  $Q$ -values of all joint actions, we cannot compute the state value using

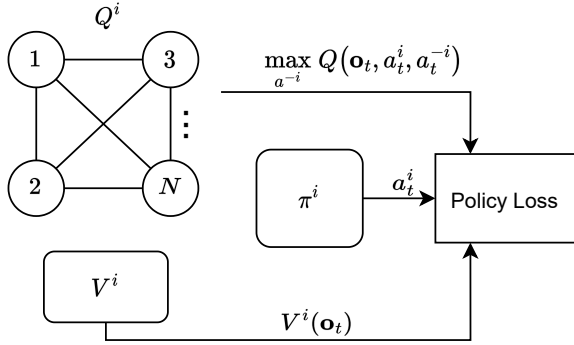


Figure 2: Architecture of the PAC-DCG algorithm. The critic computes the maximum Q-value over the joint actions.

Equation (6). Therefore, we use a separate neural network to approximate a centralised state-value function.

Figure 2 presents the architecture of the PAC-DCG algorithm. Notably, one should expect PAC to be an upper bound to the performance of PAC-DCG, since PAC-DCG approximately computes the maximum Q-value in contrast to PAC which computes the true maximum operator over the Q-values. Any other graph-based approach can be used in place of DCG, such as the Context-Aware SparsE Coordination graphs (CASEC) algorithm (Wang et al. 2022). Finally, graph-based approaches such as DCG and CASEC assume centralised execution. By using these graph-based approaches as critics, we can use them under the CTDE paradigm.

## 4 Experiments

In this section, we experimentally evaluate PAC and PAC-DCG in several multi-agent games and compare it against related baselines. We are interested in observing whether PAC achieves superior returns compared to the baselines as well as the ability of PAC’s critic to accurately represent the Q-values of the joint actions of all agents.

### 4.1 Multi-Agent Games

**Matrix Games:** Three shared-reward multi-agent matrix games proposed by Claus and Boutilier (1998): the Climbing game with two and three agents and the Penalty game. The payoff matrices of the Climbing game with two agents and the Penalty game are presented in Tables 2 and 3. The Climbing game is a two agents matrix game with three actions per agent. It has in total seven Nash equilibria (two pure-strategy and five mixed-strategy), with the joint action  $(A, A)$  being the Pareto-optimal one. We also extend the Climbing game to three agents, with one Pareto-optimal joint action  $(A, A, A)$ . We omit its payoff matrix for brevity. The Penalty game is a two agents matrix game with three actions per agent. It has in total five Nash equilibria (three of which are pure-strategy), with Pareto-optimal Nash equilibria being the joint actions  $(A, C)$  and  $(C, A)$ .

These matrix games have one or more Pareto-dominated Nash equilibria and one or more Pareto-optimal Nash equilibria.

		Agent 2		
		A	B	C
Agent 1	A	$(11, 11)^\ddagger$	$(-30, -30)$	$(0, 0)$
	B	$(-30, -30)$	$(7, 7)^\dagger$	$(0, 0)$
	C	$(0, 0)$	$(6, 6)$	$(5, 5)$

Table 2: Normal-form of the Climbing game. The game has two pure Nash equilibria, where the Pareto-optimal<sup>‡</sup> equilibrium is  $(A, A)$ .

		Agent 2		
		A	B	C
Agent 1	A	$(-100, -100)$	$(0, 0)$	$(10, 10)^\ddagger$
	B	$(0, 0)$	$(2, 2)^\dagger$	$(0, 0)$
	C	$(10, 10)^\ddagger$	$(0, 0)$	$(-100, -100)$

Table 3: Normal-form of the Penalty game. The game has three pure Nash equilibria, where the Pareto-optimal<sup>‡</sup> equilibria are  $(A, C)$  and  $(C, A)$ .

**Boulder Push:** In this game (Figure 3a), a boulder and two agents are placed in an  $8 \times 8$  grid-world. The agents must cooperate to push the boulder to the edge of the grid. Each agent has four available actions, one for moving to each direction. The boulder is pushed if all agents move in the direction that is shown by the arrows while standing on the highlighted locations. The agents receive reward 0.1 for moving the boulder, but receive reward  $-0.1$  for trying to push it on their own.

**Level-Based Foraging (LBF):** In this game (Christianos, Schäfer, and Albrecht 2020; Papoudakis et al. 2021) (Figure 3b), one food item is placed in a grid world. The agents must coordinate and move adjacent to the food and simultaneously forage it. The agents can move in four directions or attempt to forage the food. Agents receive a positive reward for coordinating and foraging the food, individual forage attempts will result in all agents receiving a reward of  $-0.6$ .

The following two games (Wang et al. 2022) have a larger number of agents and are used to evaluate PAC-DCG.

**Aloha** (Wang et al. 2022): It consists of ten agents each representing a different island which are located in a  $2 \times 5$  grid-world. The islands have a queue of messages that need to be sent. At each time step, an island can either send a message or not. If two neighbouring islands try to send a message, the messages interfere and are not sent, and all agents receive reward  $-10$ . At each time step, the agents receive  $+0.1$  for each message that is transmitted successfully. Additionally, at each time step, a new message is added to the island’s buffer with a probability of 0.6. The episode duration is 20 time steps and the goal is to optimise the number of messages that are transmitted during an episode.

**Sensors** (Wang et al. 2022): 15 agents are placed in a  $3 \times 5$  grid-world, each representing a sensor. There are also three static targets that are randomly placed at each episode. At each time step, an agent can either scan an adjacent cell with reward  $-1$ , or perform no action with 0 reward. If a target

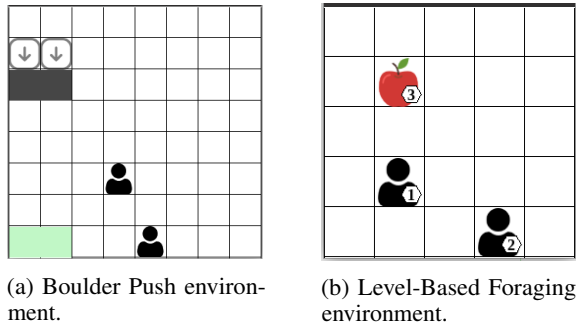


Figure 3: Boulder Push and the Level-Based Foraging environments. In both environments, the agents are penalised if they individually try to complete the task without cooperating with the other agent.

is scanned simultaneously by two or more agents then they receive reward +3. The episode duration is ten time steps, and the goal is to maximise the number of successful scans.

## 4.2 Baselines

We compare the average evaluation returns achieved by PAC against the evaluation returns achieved by four MARL algorithms: MAA2C, VDN (Sunehag et al. 2018), QMIX (Rashid et al. 2018), and QTRAN (Son et al. 2019). Gradient updates are performed at the end of each episode. Off-policy algorithms (VDN, QMIX, and QTRAN) use an experience replay to break the correlation between consecutive samples, and the gradient updates are performed by uniformly sampling a batch of 32 episodes. On-policy algorithms (MAA2C, PAC) use ten parallel processes to break the correlation between consecutive samples, and the gradient updates are performed using a batch of the ten aggregated episodes. In all algorithms, we perform the same number of gradient steps.

For consistency, PAC and all the baselines were implemented using the EPyMARL<sup>2</sup> codebase. All neural networks consist of two fully connected layers in fully-observable environments (matrix games and LBF), while the first layer of the actor is a GRU in the Boulder Push environment. The parameters of all networks are optimised using the Adam optimiser (Kingma and Ba 2015). There is no parameter sharing among the agents. The code for reproducing the experiments is included in the supplementary materials. A hyperparameter search was fairly conducted over PAC and all baselines. More information about the hyperparameter search is included in the Appendix.

## 4.3 Average Evaluation Returns

Figure 4 presents the average evaluation returns over five different seeds, which are achieved by PAC and four evaluated baselines in the aforementioned environments.

**Matrix Games:** PAC is the only method that converges to the Pareto-optimal equilibria in all games. MAA2C is the only other algorithm that solves the Penalty game, but not the Climbing games. This corroborates and reproduces the

findings of Papoudakis et al. (2021). In Fig. 5 PAC-DCG can also be seen to solve the Climbing game.

**Boulder Push:** PAC converges to higher returns compared to all the other baselines. During the first half of the training, PAC is receiving negative returns which is evidence to support that it insists on exploring promising joint actions even if they are initially penalised.

**Level-Based Foraging:** Because of the large penalty in this environment, PAC is the only algorithm to achieve returns higher than zero in both tested variations (with two and three agents). We hypothesise that this is a direct outcome of the increased representation capacity of the critic network, being able to accurately approximate the Q-values of joint actions, but also the policy gradient loss taking into account that the other agent also prefers the Pareto-optimal action.

## 4.4 Evaluation of PAC-DCG

Figure 5 presents the performance of PAC-DCG and the four baselines in three multi-agent games: Climbing, Aloha, and Sensors. We observe that PAC-DCG consistently converges to the Pareto-optimal equilibrium in the Climbing game, similarly to PAC. In the Sensors game, PAC-DCG achieves a higher number of evaluation scans compared to all baselines. Finally, in the Aloha game, PAC-DCG manages to transmit a slightly lower number of packages compared to MAA2C, but the difference is not statistically significant.

## 4.5 Evaluation on No-Conflict Games

The multi-agent games described above are fully cooperative since the reward is shared across all agents. However, PAC works in the general no-conflict case, a superset of the cooperative games. We evaluate our algorithm in the set of all structurally distinct strictly ordinal  $2 \times 2$  no-conflict games (Albrecht and Ramamoorthy 2012; Rapoport 1966). We train agents with PAC, MAA2C, and IQL for five seeds until convergence to one of the joint actions. In those runs, PAC solves all 21 games (on all five seeds) by converging to the Pareto-optimal equilibrium, while MAA2C and IQL do not consistently solve three of these games in all five tested seeds. We note that 15 of the 21 games only have one equilibrium, so it is not surprising that every algorithm solved them. The three games that were not solved by other algorithms can be seen in Table 4 and exhibit a similar structure to the stag hunt (Table 1). Note the inclusion of simpler baselines, since QMIX, VDN and QTRAN assume shared-reward games and do not apply to the general no-conflict setting.

## 4.6 Representation Capacity of PAC Critic

The learned state-action value function over the joint actions for PAC and the value decomposition algorithms VDN, QMIX, and QTRAN are important to better understand the representational capacity of the respective algorithms. Table 5 presents the Q-values of the joint actions for the four algorithms in the no-repeated Climbing game with two agents. We observe that only PAC is able to accurately represent the Q-values of all joint actions. Additionally, in the Q-values of VDN and QMIX, we observe that the first row and the first column, which are associated with action  $A$  of each agent,

<sup>2</sup><https://github.com/uo-epymarl>

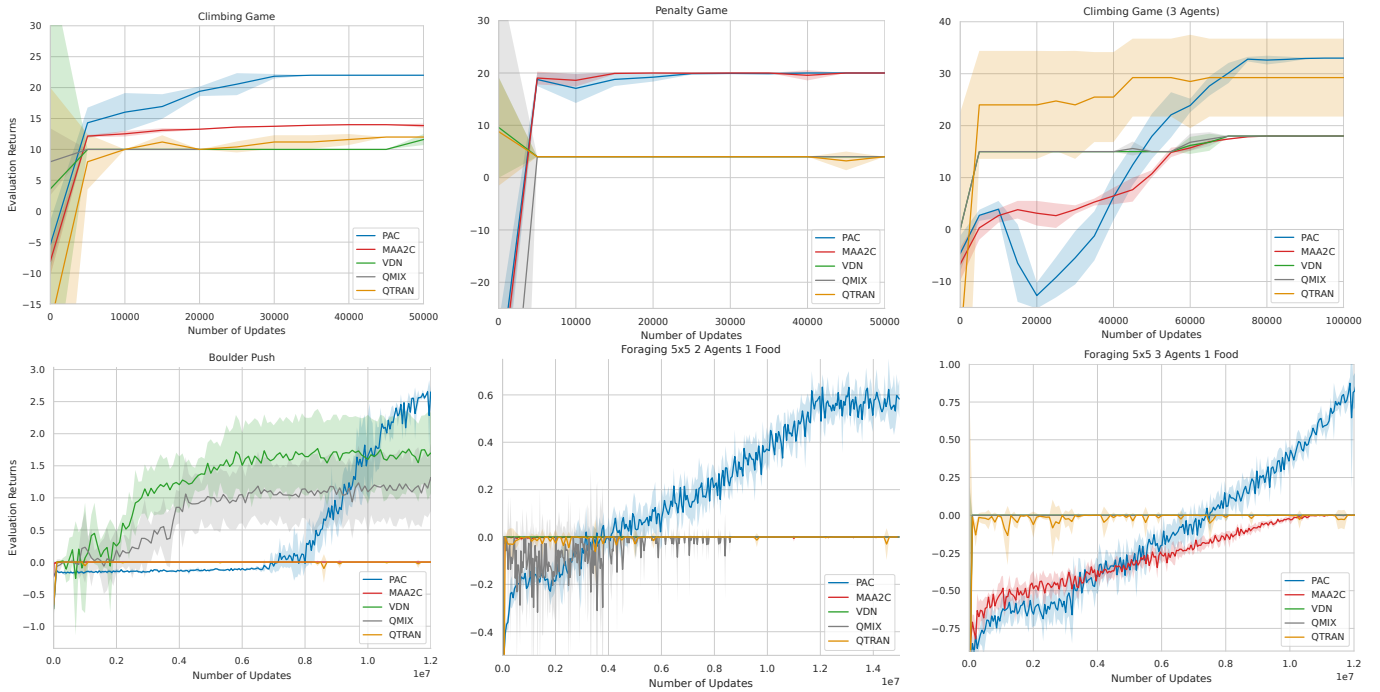


Figure 4: Average episodic evaluation returns and 95% confidence interval over 5 seeds of PAC and the evaluated baselines in five multi-agent environments.

	<i>A</i>	<i>B</i>		<i>A</i>	<i>B</i>
<i>A</i>	$(4, 4)^\ddagger$	$(1, 3)$		$(4, 4)^\ddagger$	$(1, 2)$
<i>B</i>	$(3, 1)$	$(2, 2)^\dagger$		$(3, 1)$	$(2, 2)^\dagger$

	<i>A</i>	<i>B</i>
<i>A</i>	$(4, 4)^\ddagger$	$(1, 2)$
<i>B</i>	$(2, 1)$	$(3, 3)^\dagger$

Table 4: Normal-form of the games not solved by MAA2C and IQL. The top-left game is structurally identical to the stag hunt (Table 1) and the others exhibit a similar structure. All games have two pure Nash equilibria, one that is Pareto-dominated<sup>†</sup> and one that is Pareto-optimal<sup>‡</sup>.

all contain negative values close to  $-30$ , which interestingly is the penalty for miscoordination. This is consistent with the evaluation returns presented in Figure 4, where we observe that only PAC is able to consistently converge to the Pareto-optimal Nash equilibrium in the Climbing game.

## 5 Related Work

### 5.1 Equilibrium Selection

A useful overview of relative overgeneralisation (Wiegand 2003), a term used to refer to a subset of equilibrium selection problem is discussed by Wei and Luke (2016). A clear example can be found again in the stag hunt game (Table 1), where we observe that when agent 2 selects its actions uniformly, the average return for agent 1 is 2 when it selects action A,

and 2.5 when it selects action B. At the initial stages of training, when each agent’s policy is almost uniformly initialised, and each agent will learn to select the action B which leads to higher returns. Equilibrium selection as a term in MARL is a subset of the more general issue that arises during training and is referred to as *non-stationarity* (Papoudakis et al. 2019; Hernandez-Leal et al. 2017), which is primarily caused by the uncertainty that each agent has about the policies of the other agents that are changing. Several works have been proposed to address the equilibrium selection problem that mainly focus on accurately learning the Q-value of the joint actions. One of the first approaches that learns the Q-value of the joint actions is Friend-or-Foe Q-learning (Littman 2001). They propose two different approaches; one for games where the other agents are considered friends (Friend Q-learning), and one for games where the other agents are considered foes (Foe Q-learning). In this work, we are studying no-conflict games, and therefore, we are only interested in Friend Q-learning. Assuming a game with two agents, each agent maintains a table of Q-values for all joint actions, which are updated using the following rule:

$$Q_1(s_t, a_t^1, a_t^2) \leftarrow (1 - \alpha)Q_1(s_t, a_t^1, a_t^2) + \alpha(r_t + \gamma \max_{a^{1'}, a^{2'}} Q_1(s_{t+1}, a^{1'}, a^{2'})) \quad (8)$$

where  $\alpha$  is the learning rate. Friend Q-learning is guaranteed to converge to the Pareto-optimal equilibrium if there is one, which is always the case in fully-cooperative games. More recent works focus on learning the Q-values of the joint actions, by mixing the Q-values for the actions of each individual agent (Sunehag et al. 2018; Rashid et al. 2018;

Table 5: Q-values of joint actions in the no-repeated Climbing game for PAC, VDN, QMIX and QTRAN, respectively. The actual values can be seen in Table 2 and are only approximated accurately by PAC.

	A	B	C	A	B	C	A	B	C	A	B	C
A	11.0	-30.0	0	-66.64	-29.68	-36.55	-31.15	-30.22	-30.42	-8.13	0.42	-0.08
B	-30.0	7.0	6.0	-29.96	7.0	5.96	-29.90	7.00	6.07	-17.74	-16.44	-17.22
C	0	0	5.0	-30.99	0.13	0.90	-29.93	0.03	-0.75	9.11	6.0	3.31

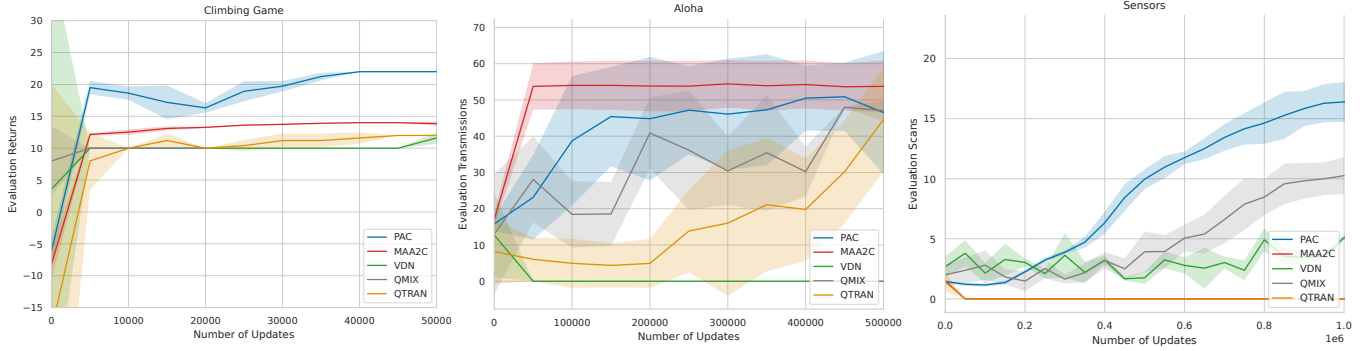


Figure 5: Average episodic evaluation performance and 95% confidence interval over 5 seeds of PAC-DCG and the evaluated baselines in the Aloha (with 10 agents) and the Sensors (with 15 agents) environments.

Son et al. 2019), which however are restricted by the representation capacity of the mixing algorithm. Another way of computing the Q-values of the joint actions is based on coordination graphs (Kok and Vlassis 2006; Castellini et al. 2019; Böhmer, Kurin, and Whiteson 2020; Wang et al. 2022), where each agent is represented by a node, while the pairwise utility between two agents is represented by an edge, and by using the message-passing algorithm in the graph the Q-value of each joint action can be computed.

## 5.2 Centralised Training Decentralised Execution

Centralised Training Decentralised Execution (CTDE) is a class of algorithms that mitigate the uncertainty each agent has about the policies of the other agents by allowing information (such as local observations and actions) to be shared during training. During execution, each agent selects their actions in a decentralised manner, only based on their own information (observation-action history). Two large classes of CTDE are the Centralised Policy Gradient Algorithms, and the Value Factorisation Algorithms. Centralised Policy Gradient Algorithms are actor-critic methods that consist of a decentralised actor and a centralised critic. During training, the critic is trained centralised to approximate the joint state (V-value) or joint state-action (Q-value) value function conditioned on the global trajectory of all agents. During execution, the decentralised actor of each agent selects its actions only based on its local trajectory. The most notable centralised policy gradient algorithms are MADDPG (Lowe et al. 2017), COMA (Foerster et al. 2018), MAA2C (Papoudakis et al. 2021) and MAPPO (Yu et al. 2021). Value Factorisation Algorithms are Q-learning-based methods, limited to cooperative environments, that factorise the global scalar reward into individual utilities for each agent. Notable works in this category are VDN (Sunehag et al. 2018) and QMIX (Rashid

et al. 2018). Both of these approaches require the *monotonicity constraint*, which practically means that the argmax of the joint Q-value is the same as the joint action that is generated if we perform the argmax operator in the individual Q-values of each agent. There are several algorithm variations in both categories that extend that focus on relaxing this constraint to be able to approximate a broader class of joint Q-values, such as QTRAN (Son et al. 2019), and QPlex (Wang et al. 2020), which however do not always yield higher returns compared to the simpler VDN, and QMIX algorithms.

## 6 Conclusion

We proposed PAC, an actor-critic MARL algorithm designed to converge to Pareto-optimal Nash equilibria in no-conflict multi-agent games. The algorithmic choices behind PAC are based on the assumption that in no-conflict games, each agent can assume that the other agents will choose the action that will lead to the Pareto-optimal equilibrium. We designed the critic in a way that facilitates efficient computation of the Q-values of all joint actions in a single forward pass. Our results indicated that PAC outperforms, in terms of achieved returns, other methods such as VDN, QMIX, and QTRAN which learn to factorise the joint Q-value into individual Q-values, as well as, MAA2C which computes a centralised state value function. Additionally, to address the computational bottleneck that is raised by the exponentially increasing number of Q-values, we proposed PAC-DCG as a scalable approximation of PAC that uses the DCG algorithm for its critic. We evaluated PAC-DCG in environments with up to 15 agents, and showed that it achieved equal or better performance compared to the baselines. In the future, we aim to explore extensions beyond no-conflict games, replacing the max operator with min-max based approaches (e.g. Littman 2001) for competitive games.

## References

- Albrecht, S. V.; and Ramamoorthy, S. 2012. Comparative Evaluation of Multiagent Learning Algorithms in a Diverse Set of Ad Hoc Team Problems. *Conference on Autonomous Agents and Multiagent Systems*.
- Albrecht, S. V.; and Stone, P. 2018. Autonomous agents modelling other agents: A comprehensive survey and open problems.
- Böhmer, W.; Kurin, V.; and Whiteson, S. 2020. Deep coordination graphs. In *International Conference on Machine Learning*, 980–991.
- Castellini, J.; Oliehoek, F. A.; Savani, R.; and Whiteson, S. 2019. The Representational Capacity of Action-Value Networks for Multi-Agent Reinforcement Learning. In *Proceedings of the 18th International Conference on Autonomous Agents and MultiAgent Systems*, 1862–1864.
- Christianos, F.; Papoudakis, G.; Rahman, A.; and Albrecht, S. V. 2021. Scaling Multi-Agent Reinforcement Learning with Selective Parameter Sharing. *Text selected: true*.
- Christianos, F.; Schäfer, L.; and Albrecht, S. V. 2020. Shared Experience Actor-Critic for Multi-Agent Reinforcement Learning. In *Advances in Neural Information Processing Systems*, volume 33, 10707–10717. Curran Associates, Inc.
- Claus, C.; and Boutilier, C. 1998. The dynamics of reinforcement learning in cooperative multiagent systems. *AAAI Conference on Artificial Intelligence*.
- Foerster, J. N.; Farquhar, G.; Afouras, T.; Nardelli, N.; and Whiteson, S. 2018. Counterfactual Multi-Agent Policy Gradients. In *Thirty-Second AAAI Conference on Artificial Intelligence*.
- Hansen, E. A.; Bernstein, D. S.; and Zilberstein, S. 2004. Dynamic programming for partially observable stochastic games. In *AAAI*, volume 4, 709–715.
- Harsanyi, J. C.; Selten, R.; et al. 1988. A general theory of equilibrium selection in games. *MIT Press Books*, 1.
- Hernandez-Leal, P.; Kaisers, M.; Baarslag, T.; and de Cote, E. M. 2017. A Survey of Learning in Multiagent Environments: Dealing with Non-Stationarity. [abs/1707.0](https://arxiv.org/abs/1707.0).
- Kingma, D. P.; and Ba, J. 2015. Adam: A Method for Stochastic Optimization. In *International Conference on Learning Representations*.
- Kok, J. R.; and Vlassis, N. 2006. Collaborative multiagent reinforcement learning by payoff propagation. *Journal of Machine Learning Research*, 7: 1789–1828.
- Littman, M. L. 2001. Friend-or-foe Q-learning in general-sum games. In *International Conference on Machine Learning, Williamstown*, 322–328.
- Lowe, R.; Wu, Y.; Tamar, A.; Harb, J.; Pieter Abbeel, O.; and Mordatch, I. 2017. Multi-Agent Actor-Critic for Mixed Cooperative-Competitive Environments. In *Advances in Neural Information Processing Systems*, volume 30, 6379–6390.
- Mnih, V.; Badia, A. P.; Mirza, M.; Graves, A.; Lillicrap, T.; Harley, T.; Silver, D.; and Kavukcuoglu, K. 2016. Asynchronous Methods for Deep Reinforcement Learning. In *International Conference on Machine Learning*, 1928–1937. PMLR. ISSN: 1938-7228.
- Papoudakis, G.; Christianos, F.; Rahman, A.; and Albrecht, S. V. 2019. Dealing with Non-Stationarity in Multi-Agent Deep Reinforcement Learning.
- Papoudakis, G.; Christianos, F.; Schäfer, L.; and Albrecht, S. V. 2021. Benchmarking Multi-Agent Deep Reinforcement Learning Algorithms in Cooperative Tasks. In *Thirty-fifth Conference on Neural Information Processing Systems Datasets and Benchmarks Track (Round 1)*.
- Rangwala, M.; and Williams, R. 2020. Learning Multi-Agent Communication through Structured Attentive Reasoning. 33.
- Rapoport, A. 1966. A taxonomy of 2x2 games. 11: 203–214.
- Rashid, T.; Samvelyan, M.; Schroeder, C.; Farquhar, G.; Foerster, J.; and Whiteson, S. 2018. QMIX: Monotonic Value Function Factorisation for Deep Multi-Agent Reinforcement Learning. In *International Conference on Machine Learning*, 4295–4304. PMLR. ISSN: 2640-3498.
- Schulman, J.; Wolski, F.; Dhariwal, P.; Radford, A.; and Klimov, O. 2017. Proximal Policy Optimization Algorithms.
- Son, K.; Kim, D.; Kang, W. J.; Hostallero, D. E.; and Yi, Y. 2019. Qtran: Learning to factorize with transformation for cooperative multi-agent reinforcement learning. In *International conference on machine learning*, 5887–5896. PMLR.
- Sunehag, P.; Lever, G.; Gruslys, A.; Czarnecki, W. M.; Zambaldi, V.; Jaderberg, M.; Lanctot, M.; Sonnerat, N.; Leibo, J. Z.; Tuyls, K.; and Graepel, T. 2018. Value-Decomposition Networks For Cooperative Multi-Agent Learning Based On Team Reward. In *Proceedings of the 17th International Conference on Autonomous Agents and MultiAgent Systems, AAMAS '18*, 2085–2087. International Foundation for Autonomous Agents and Multiagent Systems.
- Wang, J.; Ren, Z.; Liu, T.; Yu, Y.; and Zhang, C. 2020. QPLEX: Duplex Dueling Multi-Agent Q-Learning. In *International Conference on Learning Representations*.
- Wang, T.; Zeng, L.; Dong, W.; Yang, Q.; Yu, Y.; and Zhang, C. 2022. Context-Aware Sparse Deep Coordination Graphs. *International Conference on Learning Representations*.
- Wei, E.; and Luke, S. 2016. Lenient Learning in Independent-Learner Stochastic Cooperative Games. *Journal of Machine Learning Research*, 17(84): 1–42.
- Wiegand, R. P. 2003. An Analysis of Cooperative Coevolutionary Algorithms.
- Williams, R. J. 1992. Simple Statistical Gradient-Following Algorithms for Connectionist Reinforcement Learning. *Machine Learning*, 8(3-4): 229–256.
- Yu, C.; Velu, A.; Vinitzky, E.; Wang, Y.; Bayen, A.; and Wu, Y. 2021. The surprising effectiveness of ppo in cooperative, multi-agent games. *arXiv preprint arXiv:2103.01955*.

## A Implementation Details

In all algorithms, we searched the size of the hidden dimensions between 64 and 128, and the learning rate with values 0.0001, 0.0003 and 0.0005. To select the hyperparameter configurations to generate the results that were presented in Section 4, we trained all hyperparameter configurations for five different seeds for each algorithm. Then we chose the configuration that achieves the maximum evaluation return averaged over all evaluation time steps and seeds.

The target networks in all algorithms, except QTRAN, are updated using soft updates:

$$\hat{\theta}^i \leftarrow (1 - \tau)\hat{\theta}^i + \tau\theta^i$$

with  $\tau = 0.01$ . In QTRAN the parameters of the target networks are hard updated every 200 episodes. The norm of the gradient is clipped to 10 in all algorithms. In the actor-critic methods, we subtract the policy’s entropy, multiplied by an entropy coefficient, from the policy gradient loss to ensure sufficient exploration. We found it beneficial to start with a large entropy coefficient and gradually reduce it to a smaller value throughout training. In the Aloha and Sensors environments, we keep the entropy coefficient constant throughout the training. We also standardise the computed returns to have 0 mean and 1 standard deviation for all algorithms. For the TD updates of the critics, we compute the 10-step returns in all environments, except the matrix games, where the 1-step return is computed. In the off-policy methods, we use an experience replay that stores the last 50,000 episodes. Additionally, in the off-policy methods, we use epsilon-greedy exploration with the value of epsilon starting at 1 and is linearly reduced to 0.05 during the training.

The hyperparameters of PAC, PAC-DCG, MAA2C, VDN, QMIX, and QTRAN are presented in Tables 6, 7, 8, 9, 10, and 11 respectively. The code to reproduce the experiments presented is included in the supplementary material.

